IEEE Access
Multidisciplinary | Rapid Review | Open Access Journal

Received December 26, 2020, accepted March 8, 2021, date of publication April 5, 2021, date of current version April 13, 2021.

Digital Object Identifier 10.1109/ACCESS.2021.3070916

Photocurrents Recovery in GaN UV Sensors Using Microheaters at Low Temperatures

SANGHUN SHIN[1], HEEWON LEE[1], AND HONGYUN SO[1,2], (Member, IEEE)
[1]Department of Mechanical Engineering, Hanyang University, Seoul 04763, South Korea
[2]Institute of Nano Science and Technology, Hanyang University, Seoul 04763, South Korea

Corresponding author: Hongyun So (hyso@hanyang.ac.kr)

This work was supported by the Korea Institute of Energy Technology Evaluation and Planning (KETEP), granted financial resource from the Ministry of Trade, Industry and Energy of the Republic of Korea under Grant 20202000000010.

ABSTRACT At various low-temperature conditions, it is difficult to obtain an accurate sensing response due to temperature-dependent material properties such as bandgap and resistivity of semiconductors. In this study, a gallium nitride (GaN)-based ultraviolet (UV) photodetector with a microheater was demonstrated to compensate for the low-temperature effects. A parallel-type platinum microheater array was fabricated to supply thermal energy by Joule heating. In addition, a silicon oxide layer was deposited between the heater and the GaN surface, allowing an independent voltage supply. Therefore, the change in the signal level was successfully recovered to the initial state in the temperature range of $-27.4 - 11.5°C$ within $\sim 0.64\%$ error without electrical interference. This study supports an active, accurate, and reliable method for the stable measurement of UV signals in various low-temperature environments such as freezer warehouses, Antarctic research stations, and in space.

INDEX TERMS Gallium nitride, ultraviolet sensors, photocurrent, microheater, low temperature.

I. INTRODUCTION

Harsh environments, such as extreme temperatures, corrosive media, radiative and mechanical stresses, cause various damages to electronic devices and, hence, they must be utilized carefully. Due to the damages, many previous studies have reported malfunctions such as wrong sensing signal results [1], [2], thermal degradation [3]–[5], and mechanical destruction [6], [7] of the electronics. Therefore, to operate devices stably in such environments, additional technologies, including external packaging [8]–[11] methods, were used to increase sensor durability and determine exact responses. Among the harsh environments, at a low-temperature environment, material properties (i.e., bandgap [12]–[14] and resistivity [15], [16]) are changed owing to their temperature dependence, thus resulting in sensing (measurement) errors. Hence, novel methods are necessary to compensate for the low-temperature effects of microscale optoelectronics.

Nowadays, III–V compound semiconductors such as silicon carbide (SiC), gallium nitride (GaN), and aluminum nitride (AlN) have emerged as pivotal materials for electronics in harsh environments owing to their durability and robustness [17]–[19]. Among them, GaN can absorb 365-nm wavelength of incident light selectively because of the wide bandgap of 3.4 eV [20]–[22]. Therefore, GaN-based ultraviolet (UV) photodetectors that can be achieved via various solid-state device architectures have been widely studied for use in next-generation photodetector applications in harsh environments [20], [23]. In particular, various studies on metal-semiconductor-metal (MSM)-type photodetectors have emerged because of their simple fabrication process [24]–[26]. However, not only due to frost formation but also a change in the entire current scale at low temperature, the stable operation could be hindered. To solve these problems, freezing-delayed membranes [27] and a polymer lens [28] were suggested to protect the exposed surface and to enhance optical sensitivity. However, it should be noted that the delaying frost layer methods cannot be fundamental solutions because frost will eventually be generated in a saturated state. In addition, despite the gap between photocurrent and dark current (sensitivity) in responding to light, photodetectors could not recognize the stimuli because the current level cannot exceed the minimum threshold defined for the entire sensing system; thus, the device may not properly recognize the photocurrent due to the changed current level. Therefore, it not only requires protection from condensed moisture but

The associate editor coordinating the review of this manuscript and approving it for publication was Michail Kiziroglou.

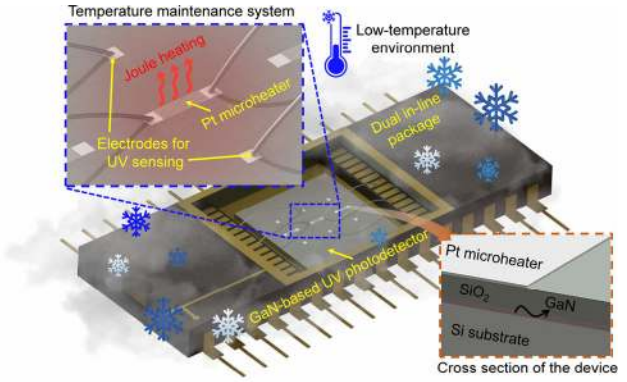

FIGURE 1. Schematic of the GaN-based UV photodetector with the microheater. Integrated Pt microheater can maintain the photodetector's surface at initial (room) temperature by Joule heating, thus initial photocurrent level can be recovered even at various low-temperature environments.

also an additional method to maintain the device temperature actively by directly controlling its temperature.

In this study, a temperature maintenance system using a platinum (Pt) microheater on an MSM-type GaN-based UV photodetector was fabricated for stable measurement of photocurrent at low temperature. Figure 1 depicts the overall schematic of the device concept. Pt microheaters were fabricated onto the sensor to maintain the temperature of the sensing area. Unlike self-heating devices [29], [30] using suspended membrane structures, a silicon dioxide (SiO_2) layer as a passivation layer exists between the Pt and GaN layers to eliminate electrical interference when the photocurrent is measured while microheaters are activated simultaneously. By doing so, the power supplies for sensing and the microheater could be biased independently. By using the system, the overall chip temperature could be maintained at room temperature by the Joule heating generated from the heater even under external low-temperature conditions. Indeed, we experimentally studied the required heating power depending on various low-temperature conditions. In addition, the current results at the recovery stage were well fitted with a theoretical equation to apply for further applications. Finally, recovery rates were calculated to demonstrate a role of microheaters compensating for the low-temperature effects. This study supports the stable operation of optoelectronics and measurement techniques using a microheater where low-temperature conditions exist such as the Arctic, space, and freezers.

II. FABRICATION

As illustrated in Fig. 2, an MSM-type GaN-based UV photodetector with a microheater was fabricated in five main steps. A 4-in. GaN-on-Si wafer (Kyma Technologies Inc.) grown by a metal organic chemical vapor deposition (MOCVD) process was prepared, as shown in Fig. 2(a). 2 μm of SiO_2 was deposited as an insulation layer on the GaN layer by a high-density plasma chemical vapor deposition (HDPCVD) process, as shown in Fig. 2(b). The SiO_2 reactive ion etching (RIE) process using octafluorocyclobutane/oxygen (C_4F_8/O_2) plasma was carried out for the electrical access to the GaN layer, as shown in Fig. 2(c). Following the previous process, Cr (10 nm) and Pt (50 nm) were deposited as a sensing electrode for better adhesion and to create Schottky contacts, respectively, as shown in Fig. 2(d). Finally, a Cr (10 nm) and Pt-based 3 × 4 parallel heater array (200 nm) was deposited onto the SiO_2 layer using an e-beam evaporator, as shown in Fig. 2(e). Each parallel microheater has nine resistive elements with a width of 15 μm and a length of 1 mm. Subsequently, the substrate was mechanically cut into 1 cm × 1 cm size, and then the microfabricated GaN-based UV photodetector was glued to a dual in-line package (DIP). In addition, the sensing electrodes and microheater were then electrically connected to the lead frame of the DIP via direct wire bonding method to create Schottky contacts and to heat the device, respectively, by utilizing a wedge bonder tool (HB05, TPT Wire Bonder GmbH & Co. KG) with aluminum wire (ALW-29S, 1%SI, Heraeus Deutschland GmbH & Co.KG). Finally, to prevent short circuit due to condensed moisture when the surrounding temperature is below 0 °C, a small amount of PDMS (polydimethylsiloxane) polymer mixture was prepared at a ratio of 10 (prepolymer): 1 (curing agent), degassed, poured onto the microheater, and cured for two days at room temperature.

III. EXPERIMENTAL SECTION

Prior to characterizing the fabricated device at low temperatures, the heating performance was evaluated by supplying a constant bias voltage to the microheater with a regulated DC power supply (TDP-305A, TOYOTech) at room temperature (∼24.5 °C). To measure the temperature distribution on the heated chip surface, an infrared (IR) camera (A65, FLIR Systems Inc.) was utilized. In advance, the emissivity of the surface was calibrated as 0.95 using a thermocouple and thermal grease for an accurate measurement. For this experiment, five different voltages were applied, and the IR images were captured for ∼200 s after operating the microheater to obtain the saturated temperature. Subsequently, transient photocurrent–voltage responses were obtained at various low-temperature conditions. Figure 3 shows images of the overall experimental setup to demonstrate the temperature recovery performance of the integrated device to the initial photocurrent level using the microheater in five different low-temperature environments. A source meter (SMU 2614B, Keithley Instruments Ltd.) was utilized to supply voltage for UV sensing and measure the transient response simultaneously. Note that the power supply for the microheater and UV sensing was conducted independently by the electrical passivation layer. In addition, a UV lamp (365 nm, UVLS-26 EL Series, UVP LLC) and a probe station (MST4000A, MSTECH Ltd.) were used to illuminate with UV light and measure the current signals in a dark environment, respectively. For each experiment cycle, the photodetector was illuminated by a 365-nm UV source of ∼0.48 mW/cm^2 intensity. The photocurrent was defined when the current reached a steady state after UV illumination. A temperature-controlled chamber (THMS600PS,

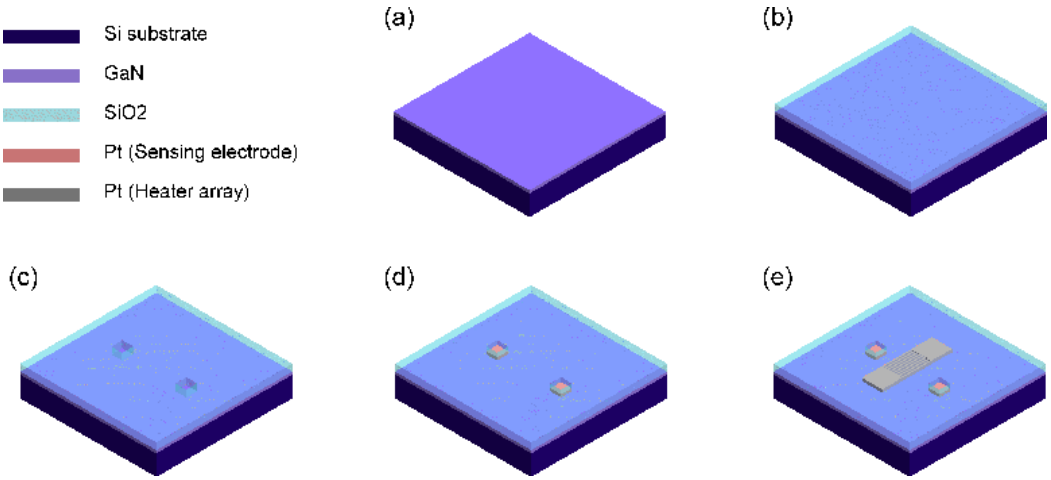

FIGURE 2. Fabrication process of the GaN-based UV photodetector with the microheater; (a) Deposition of the GaN layer on the Si wafer by MOCVD process. (b) Deposition of the SiO_2 layer onto the GaN layer by HDPCVD process for insulation. (c) RIE etching process on the SiO_2 layer. (d) Deposition of the Cr and Pt for Schottky contacts. (e) Deposition of the Pt-parallel microheater array onto the SiO_2 layer.

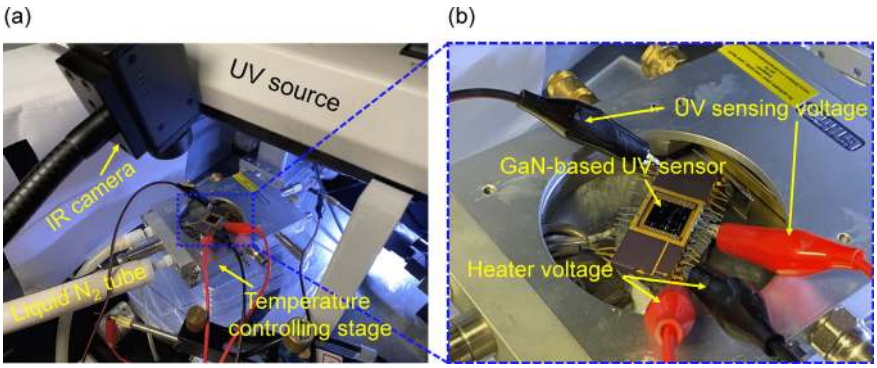

FIGURE 3. (a) Image of the experimental setup to demonstrate the GaN-based UV photodetector's performance to recover the initial photocurrent level using a microheater in low-temperature environments. (b) Magnified image of a GaN-based UV photodetector.

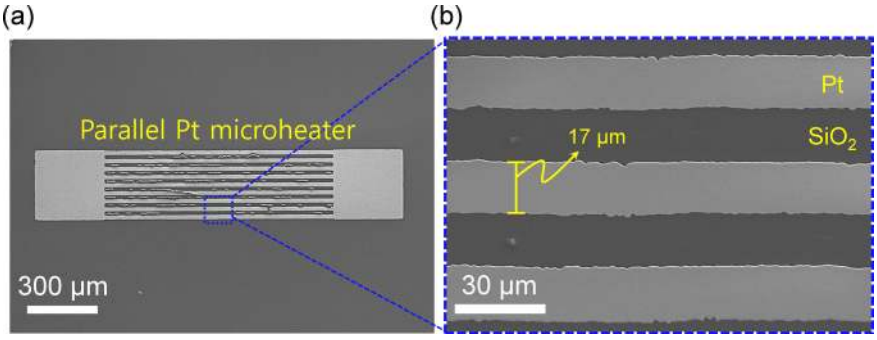

FIGURE 4. SEM images of fabricated parallel Pt microheater. (a) Top view SEM image of the microheater. (b) Magnified view of the resistive elements on SiO_2 surface.

Linkam Scientific Instruments Ltd.) was also utilized to achieve low-temperature environments. The relative humidity was measured to be 24% during the experiments.

IV. RESULTS AND DISCUSSION

As seen in Fig. 4, scanning electron microscope (SEM) images of the deposited parallel microheater were captured to demonstrate the fabrication quality. Figure 4(a) shows a top view of the fabricated parallel Pt microheater. As expected, nine parallel metal lines with two electrodes were well deposited uniformly onto the SiO_2 surface. Furthermore, the width and length of each heater line for the resistive elements were measured to be ~17 and ~977 μm, respectively, as shown in Fig. 4(b). In addition, the gap between the heater lines was ~16 μm, as measured. It should be noted that the parallel microheaters ensure stable operation even when there is potential damage because they will be able to consume electrical power despite several disconnections of the heater lines.

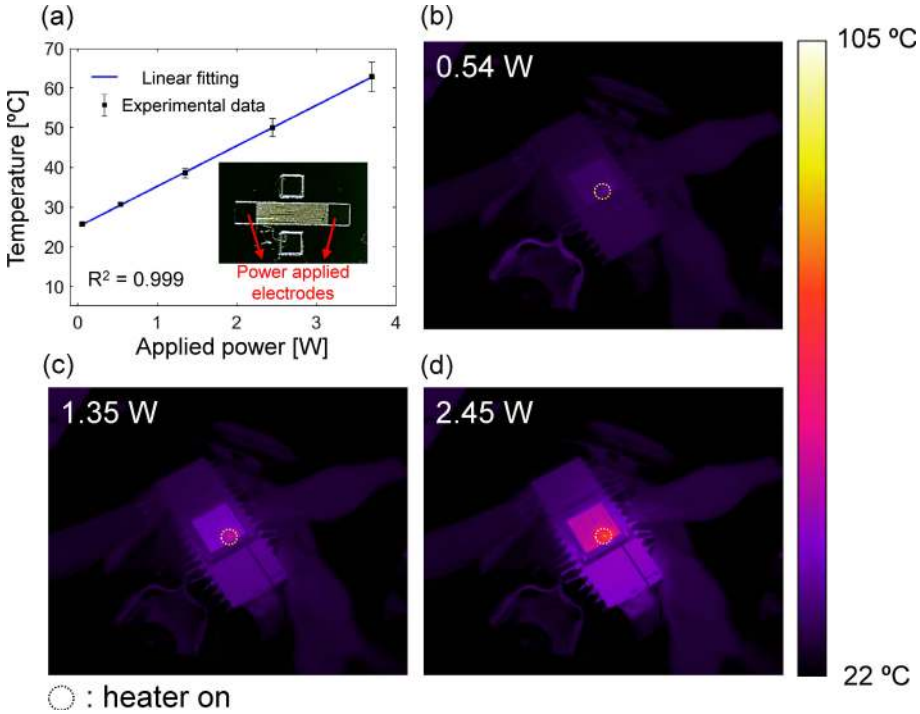

FIGURE 5. (a) Average temperature of the overall chip surface (1 cm × 1 cm) with five different applied powers at room temperature and linear fitted line. IR camera images with (b) 3 V, (c) 5 V, and (d) 7 V to demonstrate the heating performance.

Figure 5 shows the heating performance results of the microfabricated Pt parallel heater with IR camera images. For the heating bias, 1, 3, 5, 7, and 9 V were applied to the electrode that corresponded to 0.06, 0.54, 1.35, 2.45, and 3.69 W, respectively, as seen in the optical image in Fig. 5(a). In addition, the temperature was measured as 25.7, 30.64, 38.57, 50.01, and 62.82 °C, respectively. It should be noted that the fitted line matched well with the experimental data, as shown in Fig. 5(a), to predict the temperature at the other power supplies. Furthermore, Fig. 5(b), (c), and (d) show the temperature distribution with IR images when 3, 5, and 7 V were applied to the microheater, respectively. Among the heater array, the same heater located at the yellow dotted circle was used for all the following experiments in order to heat the device. Referring to the color bar, the device was gradually heated up as the applied power increased. In addition, considering the locally cured PDMS, the overall chip surface was heated evenly. It is noticeable that uniform heating ensures a stable and reliable operation from the damage caused by excessive localized heating.

To characterize the sensing performance of the sensor, the photocurrent was measured depending on the time, as depicted in Fig. 6(a). The experiments were repeated thrice for each temperature condition. For the initial stage, the current level was saturated enough from the dark current by UV illumination and maintained for 50 s. Subsequently, the device temperature was cooled down to low-temperature conditions (i.e., 11.5, 1.3, −9.5, −18.5 and −27.4 °C) for 200 s (cooling stage). Finally, the microheater was turned on to compensate for the temperature effect, and each current level was successfully recovered to the initial state in 200 s (recovery stage). It should be noted that similar trends of photocurrent and temperature plots were investigated during the initial, cooling, and recovery stages, although a sensing voltage of 1 V was applied constantly. In addition, because the device temperature was changed by the Joule heating effect from the microheater, the restoring current plot was fitted using the following equation [31], [32] for additional analysis of the recovery stage with least square curve fitting.

$$I = I_r - \alpha \times e^{-\beta t} \tag{1}$$

where I is the photocurrent level at time t, I_r is the recovered photocurrent level (i.e., final value), and α, β are fitting constants listed in Table 1. It should be noted that the average of the final photocurrent levels for 50 s was used for I_r. Furthermore, it is also noticeable that the fitting constant β serves as a time constant that is related to how fast the current is restored. The black dotted lines in Fig. 6(b) refer to the fitted curves showing well-matched results to the experimental data for each experiment for the subsequent analysis.

Figure 6(c) shows the heating power required to recover to the initial photocurrent level (I_i) from the various low temperatures. It should be noted that the well-matched fitted line can be utilized to predict the consumed power to recover its initial current level at the other temperature conditions. As shown in the IR camera image at the recovery stage in Fig. 6(c), the temperature of the chip surface was maintained around room temperature owing to the microheater despite the low surrounding temperature. Furthermore, to evaluate the recovery performance of the device, the

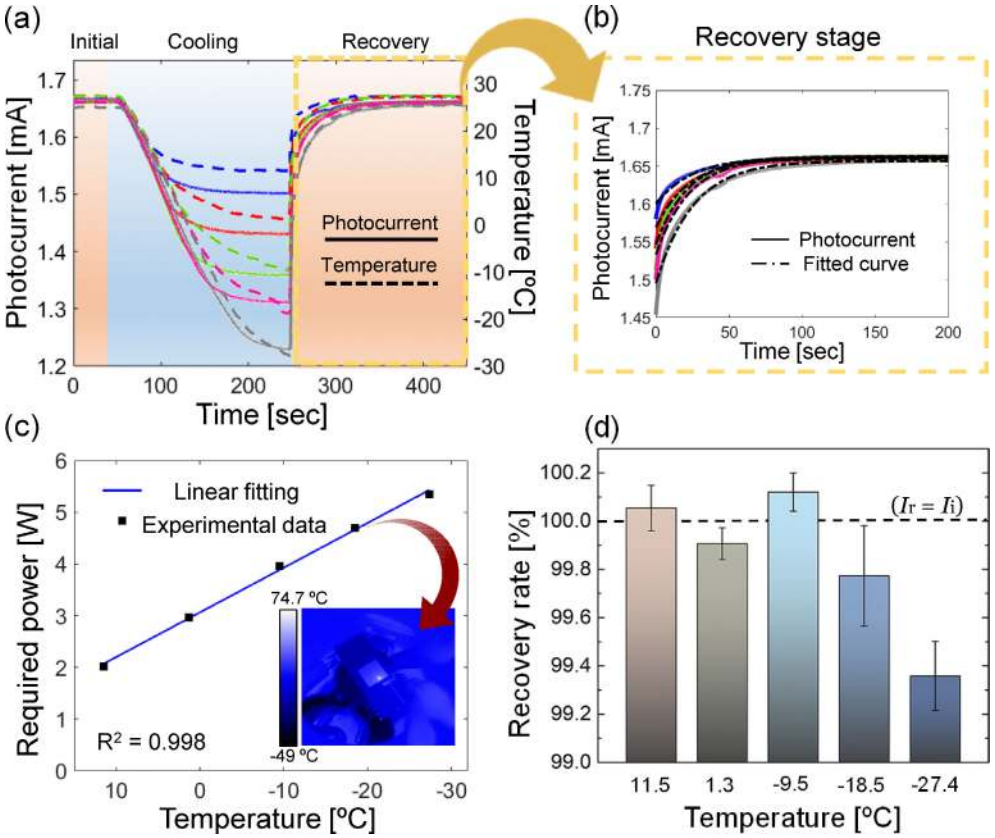

FIGURE 6. (a) Photocurrent (solid line) and temperature (dotted line) measurements at three stages including initial, cooling, and recovery stages with five different low-temperature environments. (b) Photocurrent measurements at recovery stage with fitted curves using Eq. (1). (c) Required power of the heater to recover initial photocurrent level from five different temperatures and linear fitted line. (d) Measured recovery rate by comparing the initial and final photocurrent for 50 s.

TABLE 1. Fitting constants of fitted curves to estimate photocurrents in the recovery stage.

Temperature [°C]	α [A]	$1/\beta$ [s]
11.5	6.1734×10^{-5}	25.1727
1.3	9.0474×10^{-5}	22.2082
-9.5	11.5999×10^{-5}	21.7553
-18.5	12.8436×10^{-5}	22.7397
-27.4	16.1404×10^{-5}	25.1536

recovery rate ($I_r/I_i \times 100\%$) was calculated by comparing the initial and final photocurrent for 50 s. As demonstrated in Fig. 6(d), the decrease in photocurrent due to the low-temperature effect was almost restored to the initial level (within ~0.64%) by thermal energy utilizing the microheater. Therefore, this method enables the reliable measurement of photocurrent at various low-temperature environments.

V. CONCLUSION

In summary, an active and efficient method to enhance the sensing accuracy at a low temperature of GaN-based UV photodetectors was demonstrated using a microheater with a SiO_2 insulation layer. The parallel microheater heated the overall device to compensate for the temperature effect at low-temperature conditions by Joule heating. In addition, a SiO_2 layer between the microheater and the GaN UV photodetectors realized an independent voltage supply to the heater and UV sensing. The heating performance was investigated at room temperature using an IR camera. Subsequently, photocurrent levels at various low temperatures were successfully restored to within ~0.64% error of the initial saturated values. Furthermore, to realize extended applications at various low-temperature conditions through a detailed analysis of the recovery stage, the experimental data were fitted using a theoretical equation. Consequently, the theoretical analysis of photodetector operation using a microheater was conducted in the temperature range of −27.4 to 11.5 °C. These results support the use of GaN-based UV photodetectors with microheaters at low temperatures and their theoretical analysis for future commercial photodetector applications in various low-temperature harsh environments.

ACKNOWLEDGMENT

(Sanghun Shin and Heewon Lee contributed equally to this work.)

REFERENCES

[1] B. Chen, Y. Yang, X. Xie, N. Wang, Z. Ma, K. Song, and X. Zhang, "Analysis of temperature-dependent characteristics of a 4H-SiC metal-semiconductor-metal ultraviolet photodetector," *Chin. Sci. Bull.*, vol. 57, no. 34, pp. 4427–4433, Dec. 2012.

[2] S. Siontas, D. Li, P. Liu, S. Aujla, A. Zaslavsky, and D. Pacifici, "Low-temperature operation of high-efficiency germanium quantum dot photodetectors in the visible and near infrared," *Phys. Status Solidi A*, vol. 215, no. 3, Feb. 2018, Art. no. 1700453.
[3] D. G. Yang, F. F. Wan, Z. Y. Shou, W. D. van Driel, H. Scholten, L. Goumans, and R. Faria, "Effect of high temperature aging on reliability of automotive electronics," *Microelectron. Rel.*, vol. 51, nos. 9–11, pp. 1938–1942, Sep. 2011.
[4] J. Puigcorbé, A. Vilà, J. Cerdà, A. Cirera, I. Gràcia, C. Cané, and J. R. Morante, "Thermo-mechanical analysis of micro-drop coated gas sensors," *Sens. Actuators A, Phys.*, vols. 97–98, pp. 379–385, Apr. 2002.
[5] H. W. Hou, Z. Liu, J. H. Teng, T. Palacios, and S. J. Chua, "High temperature terahertz detectors realized by a GaN high electron mobility transistor," *Sci. Rep.*, vol. 7, no. 1, May 2017, Art. no. 46664.
[6] J. Watson and G. Castro, "A review of high-temperature electronics technology and applications," *J. Mater. Sci., Mater. Electron.*, vol. 26, no. 12, pp. 9226–9235, Dec. 2015.
[7] V. Balakrishnan, H.-P. Phan, T. Dinh, D. Dao, and N.-T. Nguyen, "Thermal flow sensors for Harsh environments," *Sensors*, vol. 17, no. 9, p. 2061, Sep. 2017.
[8] V. Chidambaram, H. B. Yeung, and G. Shan, "Development of metallic hermetic sealing for MEMS packaging for Harsh environment applications," *J. Electron. Mater.*, vol. 41, no. 8, pp. 2256–2266, Aug. 2012.
[9] L. S. M. Alwis, H. Bustamante, B. Roth, K. Bremer, T. Sun, and K. T. V. Grattan, "Evaluation of the durability and performance of FBG-based sensors for monitoring moisture in an aggressive gaseous waste sewer environment," *J. Lightw. Technol.*, vol. 35, no. 16, pp. 3380–3386, Aug. 15, 2017.
[10] K. Dyrbye, T. R. Brown, and G. F. Eriksen, "Packaging of physical sensors for aggressive media applications," *J. Micromech. Microeng.*, vol. 6, no. 1, pp. 187–192, Mar. 1996.
[11] A. Hassan, Y. Savaria, and M. Sawan, "Electronics and packaging intended for emerging Harsh environment applications: A review," *IEEE Trans. Very Large Scale Integr. (VLSI) Syst.*, vol. 26, no. 10, pp. 2085–2098, Oct. 2018.
[12] K. P. O'Donnell and X. Chen, "Temperature dependence of semiconductor band gaps," *Appl. Phys. Lett.*, vol. 58, no. 25, pp. 2924–2926, Jun. 1991.
[13] W. Bludau, A. Onton, and W. Heinke, "Temperature dependence of the band gap of silicon," *J. Appl. Phys.*, vol. 45, no. 4, pp. 1846–1848, Apr. 1974.
[14] Y. P. Varshni, "Temperature dependence of the energy gap in semiconductors," *Physica*, vol. 34, no. 1, pp. 149–154, Jan. 1967.
[15] J. R. L. Fernandez, C. M. Araújo, A. F. da Silva, J. R. Leite, B. E. Sernelius, A. Tabata, E. Abramof, V. A. Chitta, C. Persson, R. Ahuja, I. Pepe, D. J. As, T. Frey, D. Schikora, and K. Lischka, "Electrical resistivity and band-gap shift of Si-doped GaN and metal-nonmetal transition in cubic GaN, InN and AlN systems," *J. Cryst. Growth*, vol. 231, no. 3, pp. 420–427, Oct. 2001.
[16] O. J. Gregory and Q. Luo, "A self-compensated ceramic strain gage for use at elevated temperatures," *Sens. Actuators A, Phys.*, vol. 88, no. 3, pp. 234–240, Jan. 2001.
[17] H. So and D. G. Senesky, "Effect of frost formation on operation of GaN ultraviolet photodetectors at low temperatures," *IEEE Sensors J.*, vol. 17, no. 15, pp. 4752–4756, Aug. 2017.
[18] M. Mehregany, C. A. Zorman, N. Rajan, and C. H. Wu, "Silicon carbide MEMS for Harsh environments," *Proc. IEEE*, vol. 86, no. 8, pp. 1594–1609, Aug. 1998.
[19] D. G. Senesky, "Wide bandgap semiconductors for sensing within extreme Harsh environments," *ECS Trans.*, vol. 50, no. 6, pp. 233–238, Mar. 2013.
[20] S. N. Mohammad, A. A. Salvador, and H. Morkoc, "Emerging gallium nitride based devices," *Proc. IEEE*, vol. 83, no. 10, pp. 1306–1355, Oct. 1995.
[21] L. Li, Z. Liu, L. Wang, B. Zhang, Y. Liu, and J.-P. Ao, "Self-powered GaN ultraviolet photodetectors with p-NiO electrode grown by thermal oxidation," *Mater. Sci. Semicond. Process.*, vol. 76, pp. 61–64, Mar. 2018.
[22] H. P. Maruska and J. J. Tietjen, "The preparation and properties of vapor-deposited single-crystal-line GaN," *Appl. Phys. Lett.*, vol. 15, no. 10, pp. 327–329, Nov. 1969.
[23] S. Chang, M. Chang, and Y. Yang, "Enhanced responsivity of GaN metal–semiconductor–metal (MSM) photodetectors on GaN substrate," *IEEE Photon. J.*, vol. 9, no. 2, pp. 1–7, Apr. 2017.
[24] E. Monroy, F. Calle, E. Muñoz, and F. Omnès, "AlGaN metal-semiconductor-metal photodiodes," *Appl. Phys. Lett.*, vol. 74, no. 22, pp. 3401–3403, May 1999.
[25] M. Gökkavas, S. Butun, T. Tut, N. Biyikli, and E. Ozbay, "AlGaN-based high-performance metal–semiconductor–metal photodetectors," *Photon. Nanostruct.-Fundam. Appl.*, vol. 5, nos. 2–3, pp. 53–62, Oct. 2007.
[26] K. Liu, M. Sakurai, and M. Aono, "ZnO-based ultraviolet photodetectors," *Sensors*, vol. 10, no. 9, pp. 8604–8634, Sep. 2010.
[27] H. So and W. Park, "Attachable freezing-delayed surfaces for ultraviolet sensing using GaN photodetector at low temperature in air," *Appl. Surf. Sci.*, vol. 473, pp. 261–265, Apr. 2019.
[28] S. Shin, B. Kang, and H. So, "Dual-surface lens with ring-shaped structures for optical tuning of GaN ultraviolet photodetectors at low temperature," *Sens. Actuators A, Phys.*, vol. 303, Mar. 2020, Art. no. 111783.
[29] J. Yun, J.-H. Ahn, D.-I. Moon, Y.-K. Choi, and I. Park, "Joule-heated and suspended silicon nanowire based sensor for low-power and stable hydrogen detection," *ACS Appl. Mater. Interfaces*, vol. 11, no. 45, pp. 42349–42357, Nov. 2019.
[30] M. Hou, H. So, A. J. Suria, A. S. Yalamarthy, and D. G. Senesky, "Suppression of persistent photoconductivity in AlGaN/GaN ultraviolet photodetectors using *in situ* heating," *IEEE Electron Device Lett.*, vol. 38, no. 1, pp. 56–59, Jan. 2017.
[31] J. Gomis, O. Galao, V. Gomis, E. Zornoza, and P. Garcés, "Self-heating and deicing conductive cement. Experimental study and modeling," *Construct. Building Mater.*, vol. 75, pp. 442–449, Jan. 2015.
[32] S.-H. Jang and Y.-L. Park, "Carbon nanotube-reinforced smart composites for sensing freezing temperature and deicing by self-heating," *Nanomater. Nanotechnol.*, vol. 8, pp. 1–8, Jan. 2018.

SANGHUN SHIN received the B.S. degree from Hanyang University, South Korea, in 2019, where he is currently pursuing the M.S. and Ph.D. degrees with the Department of Mechanical Engineering. His research interests include sensors and microsystems for extreme environments and micromachining.

HEEWON LEE is currently pursuing the B.S. degree with the Department of Mechanical Engineering, Hanyang University, South Korea. Her research interests include polymer-based microfabrication, thin film deposition process, and microsystems for biomedical applications.

HONGYUN SO (Member, IEEE) received the Ph.D. degree in mechanical engineering from the University of California at Berkeley, in 2014. In 2015, he joined as a Postdoctoral Scholar with the Department of Aeronautics and Astronautics, Stanford University. He is currently an Assistant Professor with the Department of Mechanical Engineering, Hanyang University. His research interests include design, modeling, and manufacturing of micro/nanosystems, harsh-environment sensors, and mechanical issues related to heat transfer and fluid mechanics.